Original Article

Ability of plasma-activated acetated Ringer's solution to induce A549 cell injury is enhanced by a pre-treatment with histone deacetylase inhibitors

Tetsuo Adachi,* Yumiko Matsuda, Rika Ishii, Tetsuro Kamiya, and Hirokazu Hara

Laboratory of Clinical Pharmaceutics, Gifu Pharmaceutical University, 1-25-4 Daigaku-nishi, Gifu 501-1196, Japan

(Received 1 November, 2019; Accepted 20 January, 2020; Published online 9 April, 2020)

Non-thermal plasma (NTP) is applicable to living cells and has emerged as a novel technology for cancer therapy. NTP affect cells not only by direct irradiation, but also by an indirect treatment with previously prepared plasma-activated liquid. Histone deacetylase (HDAC) inhibitors have the potential to enhance susceptibility to anticancer drugs and radiation because these reagents decondense the compact chromatin structure by neutralizing the positive charge of the histone tail. The aim of the present study was to demonstrate the advantage of the combined application of plasma-activated acetated Ringer's solution (PAA) and HDAC inhibitors on A549 cancer cells. PAA maintained its ability for at least 1 week stored at any temperature tested. Cell death was enhanced more by combined regimens of PAA and HDAC inhibitors, such as trichostatin A (TSA) and valproic acid (VPA), than by a single PAA treatment and was accompanied by ROS production, DNA breaks, and mitochondria dysfunction through a caspase-independent pathway. These phenomena induced the depletion of ATP and elevations in intracellular calcium concentrations. The sensitivities of HaCaT cells as normal cells to PAA were less than that of A549 cells. These results suggest that HDAC inhibitors synergistically induce the sensitivity of cancer cells to PAA.

Key Words: **non-thermal plasma, histone deacetylase inhibitor, DNA breaks, mitochondria dysfunction**

Plasma is often referred to as the fourth state of matter and is composed of an ionized gas of positive/negative ions, electrons, radicals, uncharged (neutral) atoms and molecules, and UV photons.[1] Based on its temperature, plasma may be categorized as thermal or non-thermal plasma (NTP). The treatment of aqueous samples with NTP results in the generation of some short- and long-lived molecules, such as reactive oxygen species (ROS) and reactive nitrogen species (RNS).[2–4] The number of potential applications of NTP discharges in medicine, particularly in cancer therapy, has increased in recent years because NTP treatments have been shown to effectively induce apoptosis in a broad range of cancer cell types.[5–7] Although biologically active targets of NTP are extremely complex with many unknown variables, the development of NTP has enabled its use in biological and medical applications. Recent studies reported that NTP affected cancer cells not only directly, but also by the indirect treatment of cells with previously prepared medium irradiated by NTP, termed plasma-activated medium (PAM), in both *in vitro* and *in vivo* experiments.[8–15] We and other researchers demonstrated that PAM functioned as a donor of reactive species, such as hydrogen peroxide (H_2O_2), and a facilitator of metals, and induced apoptosis in some cancer cell lines.[16–20] *In vivo* studies recently demonstrated that PAM significantly reduced tumor sizes in mouse models.[6,10] PAM has potential as an anti-cancer agent and will contribute to the development of a new research field "plasma pharmacy" with the accumulation of significant findings.

However, the application of PAM to the clinical phase may be impossible because culture media used in the preparation of PAM cannot be applied to medical treatments. In contrast, intravenous fluids, such as lactated Ringer's solution (Lac-R) and acetated Ringer's solution (Ac-R), are routinely used to treat patients with hypovolemia and metabolic acidosis. Therefore, the clinical application of plasma-activated liquids instead of PAM is expected. The antitumor effects of plasma-activated Lac-R (PAL) have recently been reported.[21,22] However, the properties and mechanisms underlying the functional expression of NTP-irradiated liquids have not yet been examined as extensively as those of PAM.

The basic chromatin unit is the nucleosome, comprising DNA wrapped around an octamer of histones. The structure of chromatin, open or condensed, is altered by the acetylation status of histones and directly influences gene expression. Reversible acetylation and deacetylation are regulated by histone acetyltransferases (HATs) and histone deacetylases (HDACs), respectively. HDACs enzymatically remove the acetyl group from positively charged histone lysine residues, which may then bind to negatively charged DNA. This reaction promotes the condensation of chromatin and subsequent repression of gene transcription.[23] HDAC inhibitors, such as trichostatin A (TSA) and valproic acid (VPA), loosen the chromatin structure by increasing histone acetylation. These reagents have been shown to enhance the susceptibility of chromatin to anticancer drugs and radiation.[24–31]

Lac-R and Ac-R consist of simple compositions of NaCl, KCl, $CaCl_2$, and lactate or acetate, respectively. In Ac-R, acetic acid is metabolized, even in muscle, and, thus, may be used without side effects even when liver function is reduced or lactate accumulates due to peripheral circulatory failure. The aim of the present study was to demonstrate the advantage of the combined application of plasma-activated Ac-R (PAA) and HDAC inhibitors for cancer cell death and elucidate the underlying mechanisms.

Materials and Methods

Cell culture. A549 cells (human lung adenocarcinoma epithelial cells) and HaCaT cells (human skin keratinocytes) were grown in Dulbecco's modified Eagle's medium (DMEM; Nissui Pharmaceutical Co., Tokyo, Japan) supplemented with 10% fetal

*To whom correspondence should be addressed.
E-mail: adachi@gifu-pu.ac.jp

doi: 10.3164/jcbn.19-104

calf serum (FCS), 100 units/ml penicillin, and 100 μg/ml streptomycin under an atmosphere of 5% CO_2/95% air at 37°C.

Preparation of plasma-activated solution. The experimental set-up of the NTP irradiation system used in the present study consisted of a power controller/gas flow regulator, argon gas cylinder, and plasma source head (PN-120 TPG; NU Global, Nagoya, Japan). The flow rate of argon gas was set at 2 standard liters/min (slm). PAA was prepared by exposing NTP to 6 ml of Ac-R "Veen-F Inj." (Kowa, Tokyo, Japan) in 35-mm culture dishes (Nippon Genetics, #TR4000). The distance between the NTP source and surface of the solution was fixed at L = 3 mm. The scheme is shown in Fig. 1A.

Flow cytometry. Propidium iodide (PI) has been used to detect cell damage by staining injured nuclei. A549 cells seeded at 5×10^5 cells/well on a 6-well plate (Nunc #140675) were cultured for 24 h in a CO_2 incubator. After the treatment of cells with HDAC inhibitors in DMEM-10% FCS (3 ml) for 12 h and then with PAA (3 ml) in a CO_2 incubator for 1 h, cells were washed once with ice-cold phosphate-buffered saline (PBS), treated with trypsin, and collected. After washing once with PBS, cells were suspended and stained using PI. Stained cells were analyzed using FACSVerse (BD Biosciences, San Jose, CA) with BD Cell quest Pro Software.

Measurement of cell viability. A 3-(4,5-dimethylthiazol-2-yl)-2,5-diphenyltetrazolium bromide (MTT) assay was used to assess the effects of samples on cell viability. A549 cells were seeded at 2×10^4 cells/well on a 96-well microplate (Nunc #167008), cultured for 24 h in a CO_2 incubator, and then used in experiments. Cells were treated with the indicated concentrations of TSA or VPA in DMEM-10% FCS (80 μl) for the indicated times. After the removal of HDAC inhibitors, cells were treated with PAA (80 μl) for 2 h in a CO_2 incubator, and this was provided with 100 μl of 10% FCS-added DMEM containing 500 μg/ml MTT (Sigma-Aldrich, St. Louis, MO). They were then incubated for 2 h in a CO_2 incubator. After the incubation, 100 μl of isopropanol containing 0.04 N HCl was added and then mixed thoroughly to dissolve MTT formazan. The MTT formazan produced was measured at 570 nm with a reference wavelength of 655 nm.

Assays to measure H_2O_2 concentrations. H_2O_2 concentrations in samples were assayed by a colorimetric method using 3-methyl-2-benzothiazolinone hydrazine hydrochloride, *N*,*N*-dimethylaniline, and horseradish peroxidase.[16]

Detection of acetylated histones. A549 cells were cultured in 60-mm culture dishes (Nunc #150288, seeded at 6×10^5 cells/dish) for 24 h in a CO_2 incubator and then used in experiments. Core histones were isolated from cells as described below. After cells had been treated with HDAC inhibitors in DMEM-10% FCS (3 ml) for 12 h in a CO_2 incubator, they were washed with ice-cold PBS and lysed in extraction buffer [100 mM Tris-HCl, pH 7.5, containing 0.15 M NaCl, 1.5 mM $MgCl_2$, 0.65% NP-40, 10 mM NaF, 1 mM Na_3VO_4, 20 mM β-glycerophosphate, 1 mM phenylmethylsulfonyl fluoride (PMSF), and 1 mM dithiothreitol (DTT)]. After centrifugation at 13,200 × *g* for 10 s, the pellets were mixed with 0.2 M H_2SO_4 followed by centrifugation at 13,200 × *g* for 20 min. The supernatant was mixed with 100% trichloroacetic acid and centrifuged at 13,200 × *g* for 20 min. The pellet was washed with acetone and again centrifuged at 13,200 × *g* for 5 min. The remaining histones were dissolved in 1× SDS buffer [0.45 M Tris-HCl, pH 8.8, containing 2% sodium dodecylsulfate (SDS), 6% 2-mercaptoethanol, and 0.01% bromophenol blue]. The acetylation of histones was detected by Western blotting using an anti-acetyl histone H3 or anti-acetyl histone H4 rabbit antibody (1:1,000; Millipore, Billerica, MA) as the primary antibody.

Western blotting. A549 cells were cultured in 90-mm culture dishes (Nunc #150350, seeded at 3×10^6 cells/dish) for 24 h in a CO_2 incubator and then used in experiments. Cells were treated with HDAC inhibitors in DMEM-10% FCS (8 ml) for 12 h and then with PAA (8 ml) for 2 h. Cells were washed with cold PBS, scraped, and lysed in 50 μl of lysis buffer (20 mM Tris-HCl, pH 7.4, containing 1 mM EDTA, 1 mM EGTA, 10 mM NaF, 1 mM Na_3VO_4, 20 mM β-glycerophosphate, 1 mM PMSF, 1 mM DTT, 2 μg/ml leupeptin, and 1% Triton X-100), followed by centrifugation at 17,000 × *g* for 5 min. After centrifugation, the protein concentration of the supernatant was assayed using a Bio-Rad protein assay reagent.

Extracts containing 20 μg of protein were boiled with sample buffer (62.5 mM Tris-HCl, pH 6.8, containing 2% SDS, 10% glycerol, 50 mM DTT, and 0.01% bromophenol blue) for 5 min and separated by SDS-PAGE on a 15% (w/v) polyacrylamide gel. After the proteins were transferred electrophoretically onto PVDF membranes, non-specific binding sites were blocked with PBS containing 1% bovine serum albumin (BSA). The membranes were then incubated with an anti-phospho-histone H2A.X (γH2AX) antibody (1:1,000; Cell Signaling Technology, Danvers, MA). An anti-Bcl2 antibody (1:1,000; Oncogene Research Products, La Jolla, CA), anti-Bax antibody (1:1,000; Cell Signaling Technology), and anti-actin antibody (1:1,000; Millipore) were also used as the primary antibodies.

RT-PCR. A549 cells in 90-mm culture dishes (seeded at 3×10^6 cells/dish) were cultured for 24 h in a CO_2 incubator and then used in experiments. After the treatment of cells with HDAC inhibitors in DMEM-10% FCS (8 ml) for 12 h and then with PAA (8 ml) for 2 h in a CO_2 incubator, cells were washed once with ice-cold PBS and total RNA was then extracted from cells with 1 ml of TRIzol reagent (Invitrogen, Carlsbad, CA). cDNA preparation and the reverse transcriptional-polymerase chain reaction (RT-PCR) were performed using the methods described in our previous studies.[16] The primers for RT-PCR were as follows: Rad51, sense 5'-GGAATTAGTGAAGCCAAA GCTG-3', antisense 5'-TAGCGTATGACAGATCTGGGTC-3'; Bcl2, sense 5'-GATGTCCAGCCAGCTGCACCTG-3', antisense 5'-CACAAAGGCATCCCAGCCTCC-3'; Bax, sense 5'-CAG CTCTGAGCAGATCATGA-3', antisense 5'-GCCTTGAGCACC AGTTTGCT-3'. We ascertained that there was a linear correlation between the amounts of PCR products and template cDNA under our PCR conditions. Aliquots of the PCR mixture were separated on a 2% agarose gel and stained with ethidium bromide. A densitometric analysis of the PCR products was performed with Multi Gauge ver. 3.0 (Fuji Film, Tokyo, Japan).

Detection of ROS. A549 cells seeded at 5×10^5 cells/well on a 6-well plate were cultured for 24 h in a CO_2 incubator. After the treatment of cells with HDAC inhibitors in DMEM-10% FCS (3 ml) for 12 h and then with PAA (3 ml) in a CO_2 incubator for 1 h, cells were washed twice with FluoroBrite DMEM, followed by a treatment with 1 μM dihydroethidium (Molecular Probes, Eugene, OR) for 30 min. After washing once with FluoroBrite, cells were collected and suspended. Stained cells were analyzed using FACSVerse with BD Cell quest Pro Software.

JC-1 staining. The mitochondrial membrane potential (Δψm) was detected using the fluorescence dye JC-1 (Enzo Life Sciences, Farmingdale, NY). The change from red to green fluorescence in JC-1 was used to detect a reduction in Δψm. After the treatment of A549 cells with HDAC inhibitors for 12 h and then with PAA (400 μl) in a 4-well culture plate (Nunc #176740, seeded at 1×10^5 cells/well) for 1 h in a CO_2 incubator, cells were washed once with PBS followed by the addition of 1 μM JC-1 in DMEM-10% FCS. After being incubated for 30 min in the CO_2 incubator, cells were visualized under the LSM710 confocal laser fluorescence microscope (Carl Zeiss, Gottingen, Germany).

Measurement of ATP. A549 cells were cultured in a 24-well plate (Nunc #142475, seeded at 7×10^4 cells/well) for 24 h in a CO_2 incubator and then used. After the treatment of cells with HDAC inhibitors for 12 h and then with PAA (400 μl) for 1 h in a CO_2 incubator, cells were washed with PBS followed by the

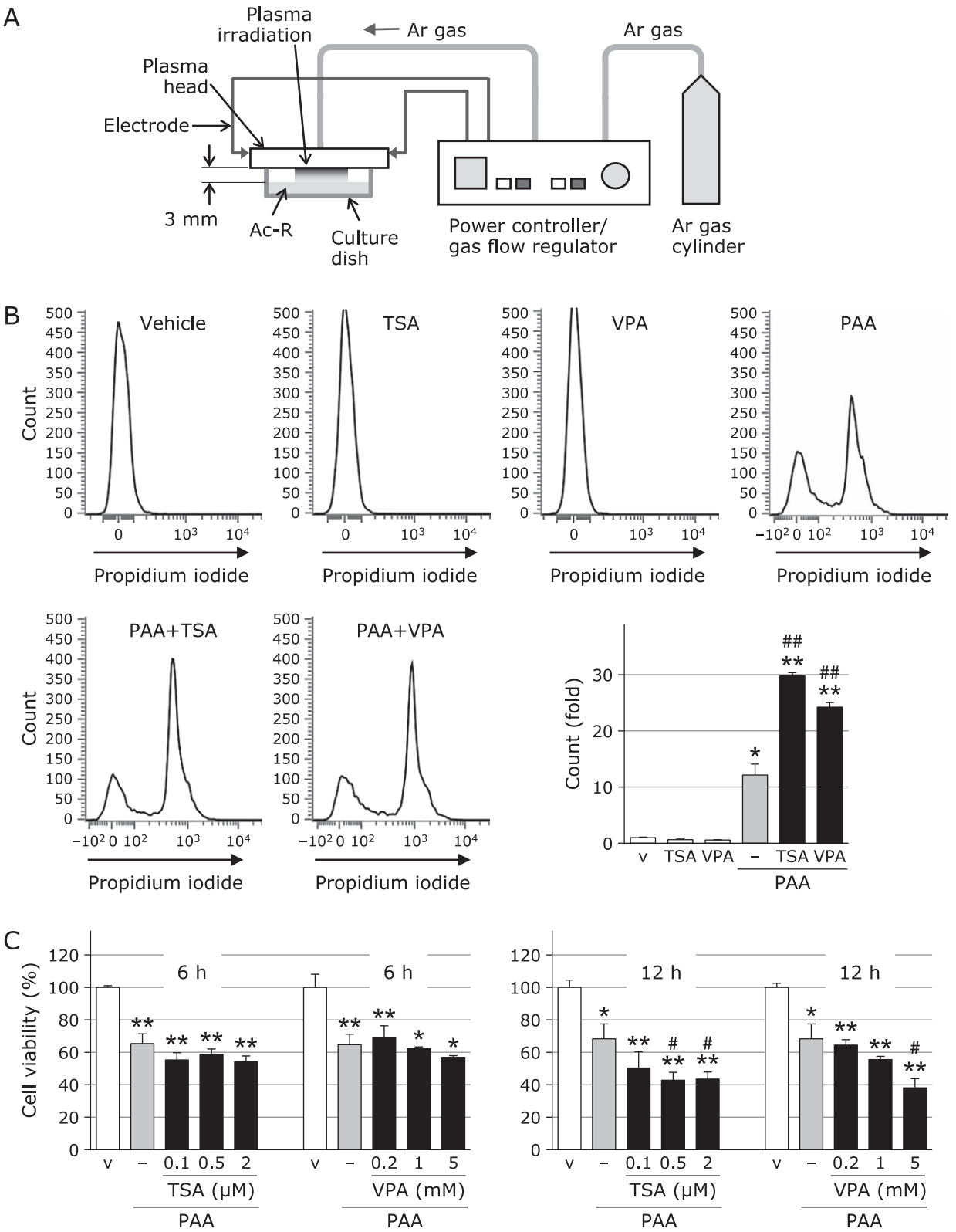

Fig. 1. Effects of HDAC inhibitors on PAA-induced cell injury. (A) A scheme depicting the experimental set-up and preparation of PAA. (B) A549 cells were pretreated with or without TSA (1 μM) or VPA (2 mM) in DMEM-10% FCS for 12 h and then with Ac-R (vehicle) or PAA for 1 h in a CO_2 incubator, and this was followed by an assay for PI-stained cells by flow cytometry as described in the Materials and methods section. PI-positive cell counts were analyzed (right). Data are shown as means ± SD (n = 3). (C) A549 cells were pretreated with or without the indicated concentrations of TSA or VPA in DMEM-10% FCS for 6 or 12 h and were then treated with Ac-R (vehicle) or PAA for 2 h in a CO_2 incubator, followed by an assay for cell viability by the MTT assay. Data are shown as means ± SD (n = 3). *p<0.05, **p<0.01 vs Ac-R only (v), $^{\#}p$<0.05, $^{\#\#}p$<0.01 vs PAA only.

doi: 10.3164/jcbn.19-104

assay for intracellular ATP using the ENLITEN ATP assay system (Promega, Madison, WI) according to the manufacturer's instructions.

Assay of intracellular calcium concentrations. A549 cells were cultured in a 96-well microplate (seeded at 2×10^4 cells/well) for 24 h in a CO_2 incubator and then used in experiments. Cells were treated with 80 μl of HDAC inhibitors for 12 h and then with PAA for 1 h in a CO_2 incubator. Cells were washed once with PBS and then subjected to an assay of intracellular calcium concentrations ($[Ca^{2+}]i$) using Calcium Kit-Fluo 4 (Dojindo, Kumamoto, Japan) according to the manufacturer's instructions.

Data analysis. Data are shown as the mean ± SD of at least three experiments. Data were analyzed using Welch's *t* test or ANOVA followed by Tukey's post-hoc test. A *p* value of less than 0.05 was considered to be significant.

Results

Effects of HDAC inhibitors on PAA-induced cell injury. NTP irradiation produced H_2O_2 in Ac-R in an irradiation time-dependent manner, and 3 min of NTP irradiation generated approximately 1 mM H_2O_2 and reduced the viability of cancer cells under our experimental conditions. Therefore, it was termed PAA. The H_2O_2 produced was considered to the main factor responsible for the effects of PAA, although other chemicals produced have also been shown to contribute to these effects.[16–20] Prepared PAA was diluted 8-fold and used in the experiments. PI is a popular nuclear and chromosome counterstain and is also commonly used to detect dead cells in a population because it is not permeable to live cells. In the present study, cell viability was measured using an assay of PI-stained cells detected by flow cytometry, as shown in Fig. 1B. The treatment of A549 cells with PAA markedly increased (12.1-fold) the number of PI-stained cells (Fig. 1B, right graph). A549 cell injury by PAA was significantly enhanced by the pretreatment of cells with HDAC inhibitors, such as TSA (2 μM, 29.8-fold) or VPA (5 mM, 24.2-fold), while the treatment with TSA or VPA only did not exert any effects. Decreases in cell viability by the treatment with PAA and the enhancing effects of TSA and VPA were also assessed using the MTT method (Fig. 1C). The pretreatment with TSA or VPA for 12 h enhanced cell injury induced by PAA, but not by the pretreatment with reagents for 6 h, and the enhancing effects of TSA and VPA were dose-dependent.

Effects of HDAC inhibitors on PAA-triggered nuclear injury. The acetylation of the histones H3 and H4 was detected after the treatment with TSA or VPA for 12 h, as shown in Fig. 2A. DNA breaks caused by the PAA treatment were detected with γH2AX in Western blotting, and were enhanced by the pretreatment with TSA or VPA, as shown in Fig. 2B. DNA fragmentation activates poly(ADP-ribose) polymerase-1 (PARP-1), which is one of the earliest cellular responses to detect DNA breaks. PARP-1 is known to catalyze the cleavage of its substrate NAD^+, which is followed by energy failure. Reductions in cell viability by the co-treatment with PAA and HDAC inhibitors were significantly suppressed by the addition of the PARP-1 inhibitor 3,4-dihydro-5-[4-(1-piperidinyl) butoxy]-1(2H)-isoquinolinone (DPQ, EMD Chemicals, San Diego, CA) (Fig. 2C).

In mammalian cells, DNA breaks are mostly repaired by either homologous recombination (HR) and/or non-homologous end-joining (NHEJ) pathways. Therefore, we examined whether an

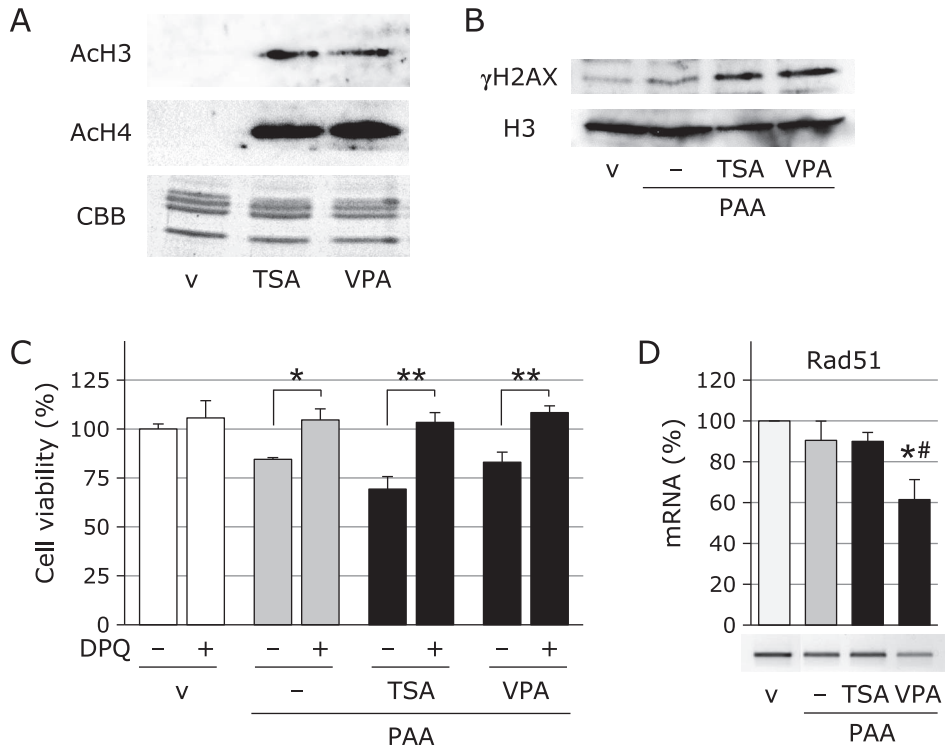

Fig. 2. Effects of HDAC inhibitors on PAA-triggered nuclear injury. (A) A549 cells were treated with or without TSA (1 μM) or VPA (2 mM) for 12 h and their acetylated histones were detected by Western blotting. Protein concentrations in samples were confirmed by Coomassie brilliant blue (CBB) staining. (B) A549 cells were pretreated with or without TSA (1 μM) or VPA (2 mM) for 12 h and were then treated with Ac-R (v) or PAA for 2 h in a CO_2 incubator, followed by Western blotting for γH2AX. (C) A549 cells were pretreated with or without TSA (1 μM) or VPA (2 mM) for 12 h and were then treated with Ac-R (v) or PAA for 2 h in the presence or absence of DPQ (10 μM), followed by an assay for cell viability by the MTT assay. Data are shown as means ± SD ($n = 3$). *$p<0.05$, **$p<0.01$. (D) A549 cells were pretreated with or without TSA (1 μM) or VPA (2 mM) for 12 h and were then treated with Ac-R (v) or PAA for 2 h in a CO_2 incubator, followed by RT-PCR for Rad51. Data are shown as means ± SD ($n = 3$). *$p<0.05$ vs Ac-R only (v), #$p<0.05$ vs PAA only.

exposure to PAA and HDAC inhibitors affects the mRNA levels of Rad51, a centrally important factor in the HR repair system, and Ku70 and Ku80, factors in the NHEJ repair system. The co-treatment with PAA and VPA significantly reduced Rad51 expression (Fig. 2D). On the other hand, the expression levels of Ku70 and Ku80 were not changed (data not shown).

Effects of HDAC inhibitors on PAA-triggered mitochondrial injury. Many mechanisms have been proposed to explain cell injury induced by plasma treatment. Previous studies reported that intracellularly accumulated ROS contribute to decreases in the mitochondrial membrane potential ($\Delta\psi m$), an indicator of mitochondrial function. ROS accumulation by the treatment with PAA was significantly enhanced by the pretreatment with TSA or VPA, as shown in Fig. 3A. The fluorescence characteristics of JC-1 changed in accordance with $\Delta\Psi m$; green fluorescence indicated a decreased membrane potential, whereas red fluorescence reflected a normal membrane potential. As shown in Fig. 3B, JC-1 green fluorescence was observed in cells co-treated with PAA and the HDAC inhibitors, TSA and VPA. The treatment with PAA only did not markedly affect JC-1 fluorescence.

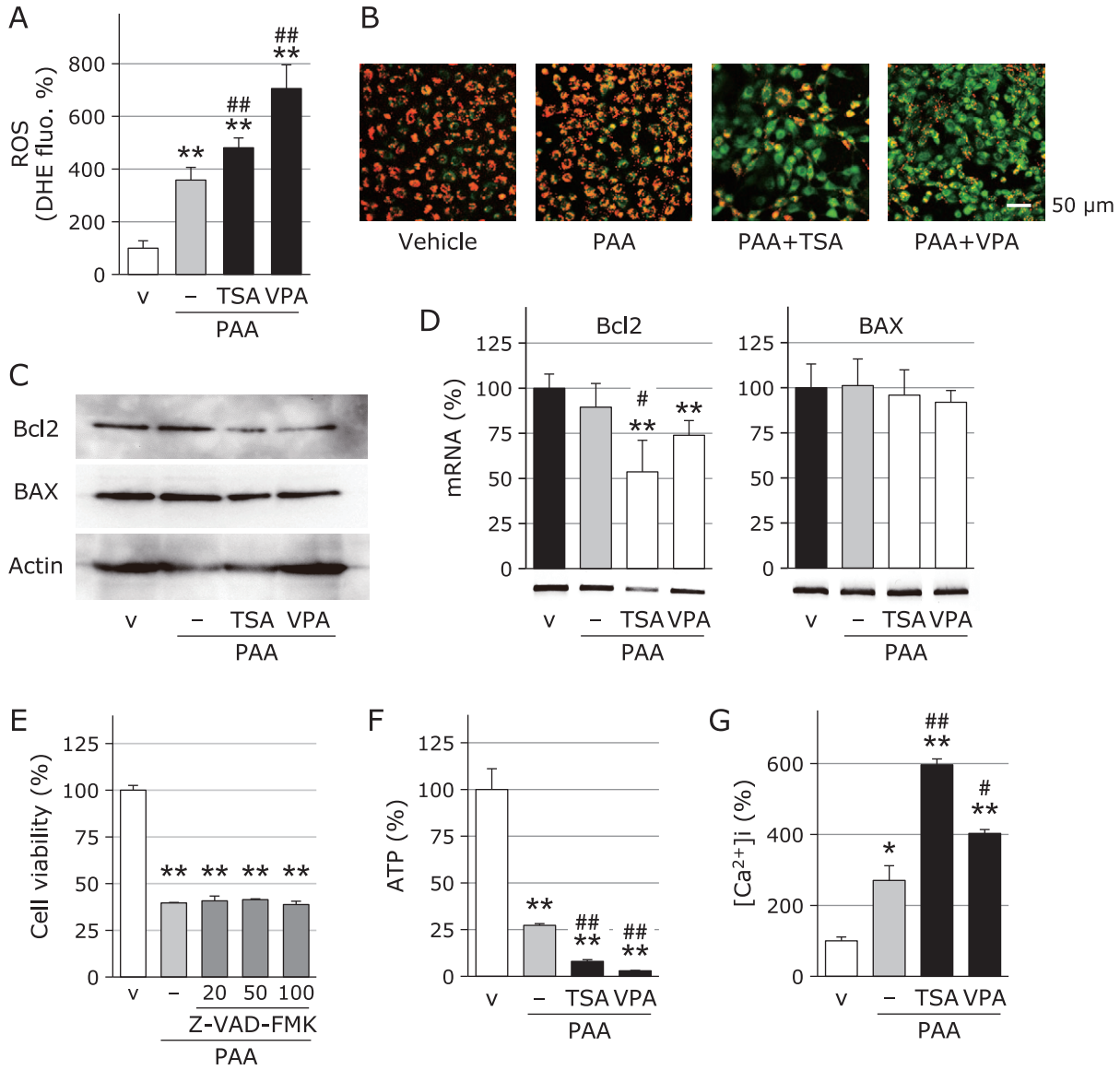

Fig. 3. Effects of HDAC inhibitors on PAA-triggered mitochondrial injury. (A) A549 cells were pretreated with or without TSA (1 μM) or VPA (2 mM) for 12 h and were then treated with Ac-R (vehicle) or PAA for 1 h in a CO_2 incubator, followed by an assay for ROS accumulation. Data are shown as means ± SD (n = 3). **p<0.01 vs Ac-R only (v), $^{\#\#}p$<0.01 vs PAA only. (B) A549 cells were pretreated with or without TSA (1 μM) or VPA (2 mM) for 12 h and were then treated with Ac-R (vehicle) or PAA for 1 h in a CO_2 incubator, followed by JC-1 staining by the method described in the "Materials and methods" section. Scale bar = 50 μm. (C) A549 cells were pretreated with or without TSA (1 μM) or VPA (2 mM) for 12 h and were then treated with Ac-R (v) or PAA for 1 h in a CO_2 incubator, followed by Western blotting. (D) A549 cells were pretreated with or without TSA (1 μM) or VPA (2 mM) for 12 h and were then treated with Ac-R (v) or PAA for 1 h in a CO_2 incubator, followed by RT-PCR for Bcl2 and Bax. Data are shown as means ± SD (n = 3). **p<0.01 vs Ac-R only (v), $^{\#}p$<0.05 vs PAA only. (E) A549 cells were treated with Ac-R (v) or PAA for 2 h in a CO_2 incubator in the presence or absence of indicated concentrations of Z-VAD-FMK (μM), followed by an assay for cell viability by the MTT assay. Data are shown as means ± SD (n = 3). **p<0.01 vs Ac-R only (v). (F) A549 cells were pretreated with or without TSA (1 μM) or VPA (2 mM) for 12 h and were then treated with Ac-R (v) or PAA for 1 h in a CO_2 incubator, followed by the assay for ATP. Data are shown as means ± SD (n = 3). **p<0.01 vs Ac-R only (v), $^{\#\#}p$<0.01 vs PAA only. (G) A549 cells were pretreated with or without TSA (1 μM) or VPA (2 mM) for 12 h and were then treated with Ac-R (v) or PAA for 1 h in a CO_2 incubator, followed by the assay for $[Ca^{2+}]i$ with the Fluo 4 fluorescence method. Data are shown as means ± SD (n = 3). *p<0.05, **p<0.01 vs Ac-R only (v), $^{\#}p$<0.05, $^{\#\#}p$<0.01 vs PAA only.

doi: 10.3164/jcbn.19-104

The expression of the mitochondrial proteins Bcl2 and Bax in A549 cells was assessed in order to elucidate the mechanisms responsible for mitochondrial injury.[32] The expression of anti-apoptotic Bcl2 was decreased by the co-treatment with PAA and HDAC inhibitors, whereas pro-apoptotic Bax remained unchanged, as shown in Fig. 3C. The mRNA level of Bcl2, but not Bax, was also significantly decreased by the co-treatment with PAA and HDAC inhibitors (Fig. 3D). We previously reported that PAM triggered cell injury through a caspase-independent pathway because we did not detect the activation of caspase, inhibition of cell injury by caspase inhibitors, or the release of cytochrome C from mitochondria to the cytosol.[16] In the present study, Z-VAD-FMK (Promega), a caspase inhibitor, did not attenuate the reduction in A549 cell viability by the PAA treatment, as shown in Fig. 3E.

Mitochondria dysfunction and the consumption of NAD^+ by the overactivation of PARP-1 resulted in energy failure, followed by the depletion of ATP. Reductions in total cellular ATP levels were detected in cells treated with PAA and were significantly enhanced by the pretreatment with TSA or VPA (Fig. 3F). These phenomena induce the influx of Ca^{2+} as the final reaction to cell death. PAA-induced elevations in $[Ca^{2+}]i$ were significantly enhanced by the pretreatment with TSA or VPA, as shown in Fig. 3G.

Effects of HDAC inhibitors and PAA on the viability of normal cells. The PAA treatment only negligibly suppressed the viability of HaCaT cells as normal cells, and HDAC inhibitors slightly enhanced the effects of PAA, as shown in Fig. 4. The sensitivity of HaCaT cells to PAA with or without a HDAC inhibitor pretreatment was significantly less than that of A549 cells.

Duration of PAA activity. We previously reported that the ability of PAM to suppress the viability of A549 cells was not altered by 7 days of storage at –80°C, whereas its activity was decreased by storage at –30°C, 4°C, and room temperature.[16] In the present study, the ability of PAA to suppress the viability of A549 cells was almost unchanged, even when it was stored at any temperature, as shown in Fig. 5A upper graph. The results obtained showed that the H_2O_2 concentration in PAA was not changed over 7 days at any temperature (Fig. 5A, lower graph). We compared changes in the ability to suppress cell viability and H_2O_2 concentrations over 7 days between PAA and PAM, and confirmed decreases by PAM stored at –30°C, 4°C, and room temperature (Fig. 5B).

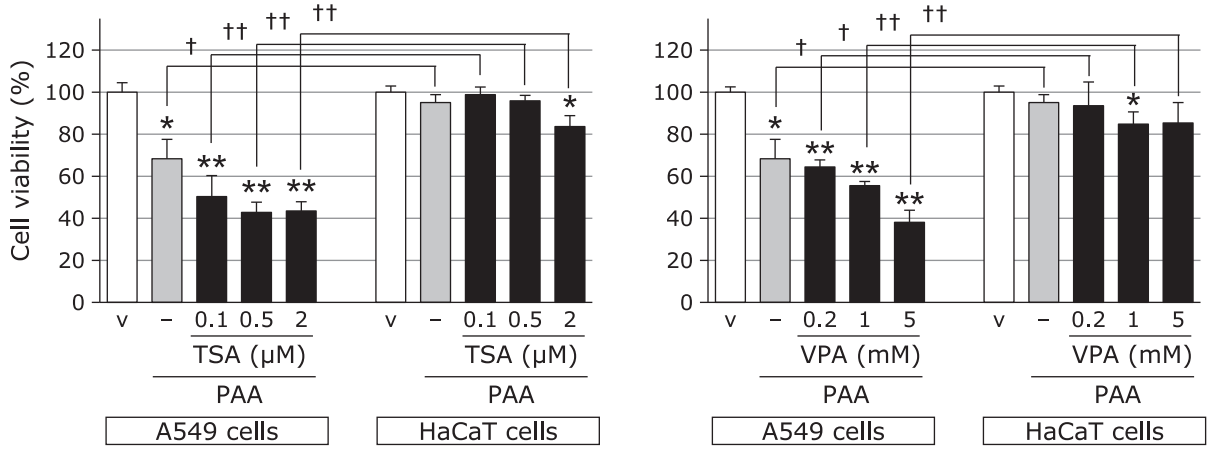

Fig. 4. Effects of HDAC inhibitors and PAA on the viability of normal cells. HaCaT cells were pretreated with or without the indicated concentrations of TSA or VPA in DMEM-10% FCS for 12 h and were then treated with Ac-R (vehicle) or PAA for 2 h in a CO_2 incubator, followed by an assay for cell viability by the MTT assay. Data for A549 cells are quoted from Fig. 1C right. Data are shown as means ± SD (n = 3). **p<0.01, *p<0.05 vs Ac-R only (v), $^{\dagger}p$<0.05, $^{\dagger\dagger}p$<0.01 between A549 cells and HaCaT cells.

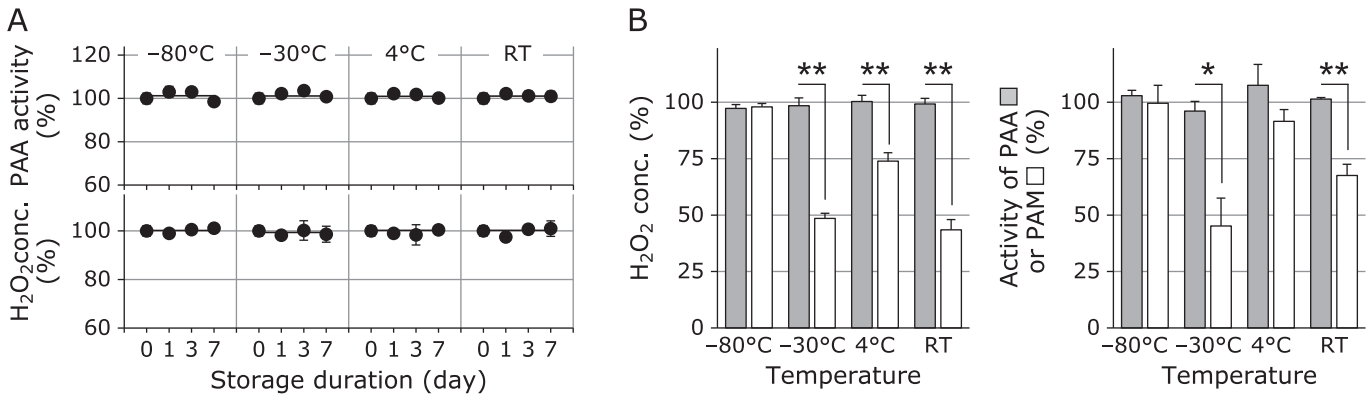

Fig. 5. Duration of PAA activity. (A) Prepared PAA was stored at –80°C, –30°C, 4°C, or room temperature (RT) for 1, 3, or 7 days, followed by an assay to measure H_2O_2 concentrations (lower) and the ability to suppress A549 cell viability (upper). Data are shown as means ± SD (n = 3). (B) Prepared PAA (gray columns) and PAM (open columns) were stored at –80°C, –30°C, 4°C, or room temperature (RT) for 7 days, followed by an assay to measure H_2O_2 concentrations (left) and the ability to suppress A549 cell viability (right). Data are shown as means ± SD (n = 3). *p<0.05, **p<0.01 between PAA and PAM. Activity of PAA (or PAM) is shown as the ratio (%) of reduction rate of cell viability by the treatment with PAA (or PAM) stored to reduction rate of cell viability by the treatment with PAA (or PAM) prepared immediately before.

Discussion

The present results demonstrated that HDAC inhibitors in combination with plasma-activated liquid PAA enhanced anticancer effects in A549 lung adenocarcinoma cells. Some types of lung cancers are unresponsive to chemotherapeutics, emphasizing the need for novel therapeutic approaches. HDAC inhibitors are a class of chemotherapeutic agent that change gene expression and inhibit the growth of cancer cells. Moreover, recent studies reported that epigenetics are closely related to the occurrence and metastasis of tumors.[33] Lung cancer cells that become resistant to death exhibit HDAC activity, and HDAC inhibitors have been used to enhance the therapeutic effects of chemotherapy and radiotherapy.[24–31]

Recent studies reported that NTP affects cells not only directly, but also indirectly in cells treated with previously prepared PAM.[8–11] Cancer therapy with PAM may be beneficial, particularly against chemoresistant cells, and more effective when used in combination with selected antitumor drugs.[6] However, cell culture media used for the preparation of PAM cannot be used for medical treatments. In contrast, intravenous fluids, such as Ac-R, are routinely used to treat patients. We observed that PAA suppressed the viability of A549 cells. In the present study, enhancements in the ability of PAA by the combination with HDAC inhibitors were examined because the ability of PAA alone was insufficient. The pretreatment of cells with TSA or VPA significantly enhanced the ability of PAA, as shown in Fig. 1. HDAC inhibitors increased acetylated lysine and/or arginine residues in the N-terminal tail of histones. We confirmed the abilities of TSA and VPA on the acetylation of the histones H3 and H4 (Fig. 2A). The acetylation of histones by the above HDAC inhibitors de-condensed the compact chromatin structure by neutralizing the positive charge of the histone tail,[34] and has been shown to increase the susceptibility of cells to radiation and anticancer drugs targeting DNA. Loose and neutralized chromatin may also be vulnerable to attack by PAA and its active species. DNA breaks caused by the co-treatment with PAA and HDAC inhibitors were detected with γH2AX Western blotting (Fig. 2B). Furthermore, HDAC inhibitors are known to reduce the DNA repair ability by down-regulating the HR or NHEJ pathways.[35,36] The treatment with VPA significantly and preferentially down-regulated the mRNA level of Rad51, a centrally important factor in HR (Fig. 2D), but not those of NHEJ proteins in A549 cells. PARP-1 is activated by a reaction with DNA nicks and catalyzed the cleavage of NAD^+ into nicotinamide and ADP-ribose to form large amounts of polyADPR. This reaction leads to the consumption of NAD^+ and depletion of ATP. Moreover, polyADPR may translocate to the mitochondria and induce its dysfunction.

Intracellularly accumulated ROS contributed to the decline in mitochondrial membrane function.[37] The increase in ROS may be due to oxidative phosphorylation uncoupling, and HDAC inhibitors are known to induce ROS production in mitochondria.[38] TSA or VPA markedly induced ROS production and reduced $\Delta\psi m$ (Fig. 3A and B). PAA contains H_2O_2 and synergistically enhances oxidative stress with HDAC inhibitors. Significant reductions in anti-apoptotic Bcl2 levels by the treatment with PAA and its enhancement with TSA or VPA (Fig. 3C and D) amplified mitochondrial dysfunction. We did not detect the inhibition of cell injury by caspase inhibitors or the up-regulation of Bax (Fig. 3C–E). These results suggest that PAA-triggered cell injury is a caspase-independent pathway similar to PAM-triggered cell injury, as shown in our previous study.[16] Moreover, a caspase-independent mechanism was recently reported for cell death caused by non-thermal plasma.[39–41] We observed PAA-induced disturbances in the nuclear-mitochondrial compartment in A549 cells in the present study, similar to PAM-induced injury,[16] and this depleted ATP, which exhausted the energy supply, and eventually allowed the influx of extracellular Ca^{2+} (Fig. 3F and G). However, the ROS-triggered disturbance of the intracellular signaling mechanism to induce cellular dysfunction may differ between PAA- and PAM-induced cell death. Tanaka *et al.*[42] recently reported the intracellular molecular mechanism responsible for cell death between PAM-treated and PAL-treated glioblastoma using microarray analyses and RT-PCR. PAM and PAL both down-regulated phosphor-AKT; however, the underlying mechanisms differed. PAM up-regulated a stress-inducing signaling pathway, whereas PAL down-regulated the survival and proliferation signaling network.

Cell selectivity is an important aspect for the application of PAA to cancer therapy. Similar to previous findings,[43,44] we herein found that normal cells were generally more resistant to plasma-treated liquids than cancer cell lines (Fig. 4). We also suggested that differences in the dependence of glycolysis on energy demand, intracellular levels of mobile zinc, and sensitivity to aconitase between cancer cells and normal cells contribute to the cell selectivity of PAM.[19]

The stability of PAA during its storage is another factor that influences its potential for clinical applications. PAA maintained its ability to suppress the viability of A549 cells for at least 1 week without the decomposition of H_2O_2 at any temperature tested (Fig. 5). This result is completely different from that of PAM and clearly demonstrates the advantages of PAA.[16] Simple compositions of inorganic salts and acetate in PAA may be responsible, whereas PAM consists of inorganic salt, glucose, carbonic acids, amino acids, and vitamins.

The supply of "safe plasma medicine" to patients is of critical importance. The biggest advantage of cancer treatments with NTP-activated liquid over direct plasma exposure is that NTP-activated liquid may be prepared in advance for clinical cancer therapy and provided to unspecified patients as a "medicine". Moreover, NTP-activated liquid has potential as an advantageous clinical tool for cancer therapy; it represents a useful treatment for larger injured areas, for example, as an intraperitoneal treatment for the micrometastatic dissemination of cancer cells.[11,13,45] Ringer's solutions are used as solvents for anticancer drugs administered intraperitonially or intraperitoneal washes other than electrolyte solutions for intravenous infusion.[46–49] The intraperitoneal administration of PAL was recently reported to suppress the growth of pancreatic cancer cells in a peritoneal dissemination mouse tumor model *in vivo*.[22] Although further investigations are needed, the results of the present study provide evidence for the anti-tumor effects of the synergism between PAA and HDAC inhibitors as well as its potential for clinical applications.

Acknowledgments

This study was supported in part by JSPS KAKENHI to TA, Grant Numbers 16K08914.

Conflict of Interest

No potential conflicts of interest were disclosed.

References

1 Kalghatgi S, Kelly CM, Cerchar E, *et al*. Effects of non-thermal plasma on mammalian cells. *PLoS One* 2011; **6**: e16270.

2 Panngom K, Baik KY, Nam MK, Han JH, Rhim H, Choi EH. Preferential killing of human lung cancer cell lines with mitochondrial dysfunction by nonthermal dielectric barrier discharge plasma. *Cell Death Dis* 2013; **4**: e642.

3 Vandamme M, Robert E, Lerondel S, *et al*. ROS implication in a new anti-

doi: 10.3164/jcbn.19-104

tumor strategy based on non-thermal plasma. *Int J Cancer* 2012; **130**: 2185–2194.
4 Kaneko T, Sasaki S, Takashima K, Kanzaki M. Gas-liquid interfacial plasmas producing reactive species for cell membrane permeabilization. *J Clin Biochem Nutr* 2017; **60**: 3–11.
5 Keidar M, Walk R, Shashurin A, *et al*. Cold plasma selectivity and the possibility of a paradigm shift in cancer therapy. *Br J Cancer* 2011; **105**: 1295–1301.
6 Utsumi F, Kajiyama H, Nakamura K, *et al*. Effect of indirect nonequilibrium atmospheric pressure plasma on anti-proliferative activity against chronic chemo-resistant ovarian cancer cells *in vitro* and *in vivo*. *PLoS One* 2013; **8**: e81576.
7 Tanaka H, Mizuno M, Toyokuni S, *et al*. Cancer therapy using non-thermal atmospheric pressure plasma with ultra-high electron density. *Phys Plasma* 2015; **22**: 122004.
8 Tanaka H, Mizuno M, Ishikawa K, *et al*. Plasma-activated medium selectively kills glioblastoma brain tumor cells by down-regulating a survival signaling molecule, AKT kinase. *Plasma Med* 2011; **1**: 265–277.
9 Hoentsch M, von Woedtke T, Weltmann K-D, Nebe JB. Time-dependent effects of low-temperature atmospheric-pressure argon plasma on epithelial cell attachment, viability and tight junction formation *in vitro*. *J Phys D Appl Phys* 2012; **45**: 025206.
10 Hattori M, Yamada S, Torii K, *et al*. Effectiveness of plasma treatment on pancreatic cancer cells. *Int J Oncol* 2015; **47**: 1655–1662.
11 Utsumi F, Kajiyama H, Nakamura K, *et al*. Variable susceptibility of ovarian cancer cells to non-thermal plasma-activated medium. *Oncol Rep* 2016; **35**: 3169–3177.
12 Wada N, Ikeda JI, Tanaka H, *et al*. Effect of plasma-activated medium on the decrease of tumorigenic population in lymphoma. *Pathol Res Pract* 2017; **213**: 773–777.
13 Nakamura K, Peng Y, Utsumi F, *et al*. Novel intraperitoneal treatment with non-thermal plasma-activated medium inhibits metastatic potential of ovarian cancer cells. *Sci Rep* 2017; **7**: 6085.
14 Ikeda JI, Tanaka H, Ishikawa K, Sakakita H, Ikehara Y, Hori M. Plasma-activated medium (PAM) kills human cancer-initiating cells. *Pathol Int* 2018; **68**: 23–30.
15 Chauvin J, Gibot L, Griseti E, *et al*. Elucidation of *in vitro* cellular steps induced by antitumor treatment with plasma-activated medium. *Sci Rep* 2019; **9**: 4866.
16 Adachi T, Tanaka H, Nonomura S, Hara H, Kondo S, Hori M. Plasma-activated medium induced A549 cell injury by a spiral apoptotic cascade involving the mitochondrial-nuclear network. *Free Radic Biol Med* 2015; **79**: 28–44.
17 Hara H, Taniguchi M, Kobayashi M, Kamiya T, Adachi T. Plasma-activated medium-induced intracellular zinc liberation causes death of SH-SY5Y cells. *Arch Biochem Biophys* 2015; **584**: 51–60.
18 Adachi T, Nonomura S, Horiba M, *et al*. Iron stimulates plasma-activated medium-induced A549 cell injury. *Sci Rep* 2016; **6**: 20928.
19 Hara H, Sueyoshi S, Taniguchi M, Kamiya T, Adachi T. Differences in intracellular mobile zinc levels affect susceptibility to plasma-activated medium-induced cytotoxicity. *Free Radic Res* 2017; **51**: 306–315.
20 Boehm D, Curtin J, Cullen PJ, Bourke P. Hydrogen peroxide and beyond-the potential of high-voltage plasma-activated liquids against cancerous cells. *Anticancer Agents Med Chem* 2018; **18**: 815–823.
21 Tanaka H, Nakamura K, Mizuno M, *et al*. Non-thermal atmospheric pressure plasma activates lactate in Ringer's solution for anti-tumor effects. *Sci Rep* 2016; **6**: 36282.
22 Sato Y, Yamada S, Takeda S, *et al*. Effect of plasma-activated lactated Ringer's solution on pancreatic cancer cells *in vitro* and *in vivo*. *Ann Surg Oncol* 2018; **25**: 299–307.
23 Lane AA, Chabner BA. Histone deacetylase inhibitors in cancer therapy. *J Clin Oncol* 2009; **27**: 5459–5468.
24 Kim MS, Blake M, Baek JH, Kohlhagen G, Pommier Y, Carrier F. Inhibition of histone deacetylase increases cytotoxicity to anticancer drugs targeting DNA. *Cancer Res* 2003; **63**: 7291–7300.
25 Gong Y, Ni ZH, Zhang X, Chen XH, Zou ZM. Valproic acid enhances the anti-tumor effect of (–)-gossypol to Burkitt lymphoma Namalwa cells. *Biomed Environ Sci* 2015; **28**: 773–777.
26 Sharma NL, Groselj B, Hamdy FC, Kiltie AE. The emerging role of histone deacetylase (HDAC) inhibitors in urological cancers. *BJU Int* 2013; **111**: 537–542.
27 Mrkvicova A, Chmelarova M, Peterova E, *et al*. The effect of sodium butyrate and cisplatin on expression of EMT markers. *PLoS One* 2019; **14**: e0210889.
28 Chie EK, Shin JH, Kim JH, Kim HJ, Kim IA, Kim IH. *In vitro* and *in vivo* radiosensitizing effect of valproic acid on fractionated irradiation. *Cancer Res Treat* 2015; **47**: 527–533.
29 Chinnaiyan P, Cerna D, Burgan WE, *et al*. Postradiation sensitization of the histone deacetylase inhibitor valproic acid. *Clin Cancer Res* 2008; **14**: 5410–5415.
30 Groselj B, Sharma NL, Hamdy FC, Kerr M, Kiltie AE. Histone deacetylase inhibitors as radiosensitisers: effects on DNA damage signalling and repair. *Br J Cancer* 2013; **108**: 748–754.
31 Moertl S, Payer S, Kell R, Winkler K, Anastasov N, Atkinson MJ. Comparison of radiosensitization by HDAC inhibitors CUDC-101 and SAHA in pancreatic cancer cells. *Int J Mol Sci* 2019; **20**. pii: E3259.
32 Lindsay J, Esposti MD, Gilmore AP. Bcl-2 proteins and mitochondria-specificity in membrane targeting for death. *Biochim Biophys Acta* 2011; **1813**: 532–539.
33 Thomson TM, Balcells C, Cascante M. Metabolic plasticity and epithelial-mesenchymal transition. *J Clin Med* 2019; **8**. pii: E967.
34 Culley KL, Hui W, Barter MJ, *et al*. Class I histone deacetylase inhibition modulates metalloproteinase expression and blocks cytokine-induced cartilage degradation. *Arthritis Rheum* 2013; **65**: 1822–1830.
35 Shoji M, Ninomiya I, Makino I, *et al*. Valproic acid, a histone deacetylase inhibitor, enhances radiosensitivity in esophageal squamous cell carcinoma. *Int J Oncol* 2012; **40**: 2140–2146.
36 Adimoolam S, Sirisawad M, Chen J, Thiemann P, Ford JM, Buggy JJ. HDAC inhibitor PCI-24781 decreases RAD51 expression and inhibits homologous recombination. *Proc Natl Acad Sci U S A* 2007; **104**: 19482–19487.
37 Levraut J, Iwase H, Shao ZH, Vanden Hoek TL, Schumacker PT. Cell death during ischemia: relationship to mitochondrial depolarization and ROS generation. *Am J Physiol Heart Circ Physiol* 2003; **284**: H549–H558.
38 Sun S, Han Y, Liu J, *et al*. Trichostatin A targets the mitochondrial respiratory chain, increasing mitochondrial reactive oxygen species production to trigger apoptosis in human breast cancer cells. *PLoS One* 2014; **9**: e91610.
39 Saito K, Asai T, Fujiwara K, *et al*. Tumor-selective mitochondrial network collapse induced by atmospheric gas plasma-activated medium. *Oncotarget* 2016; **7**: 19910–19927.
40 Conway GE, Casey A, Milosavljevic V, *et al*. Non-thermal atmospheric plasma induces ROS-independent cell death in U373MG glioma cells and augments the cytotoxicity of temozolomide. *Br J Cancer* 2016; **114**: 435–443.
41 Conway GE, He Z, Hutanu AL, *et al*. Cold Atmospheric Plasma induces accumulation of lysosomes and caspase-independent cell death in U373MG glioblastoma multiforme cells. *Sci Rep* 2019; **9**: 12891.
42 Tanaka H, Mizuno M, Katsumata Y, *et al*. Oxidative stress-dependent and -independent death of glioblastoma cells induced by non-thermal plasma-exposed solutions. *Sci Rep* 2019; **9**: 13657.
43 Utsumi F, Kajiyama H, Nakamura K, Tanaka H, Hori M, Kikkawa F. Selective cytotoxicity of indirect nonequilibrium atmospheric pressure plasma against ovarian clear-cell carcinoma. *Springerplus* 2014; **3**: 398.
44 Guerrero-Preston R, Ogawa T, Uemura M, *et al*. Cold atmospheric plasma treatment selectively targets head and neck squamous cell carcinoma cells. *Int J Mol Med* 2014; **34**: 941–946.
45 Kajiyama H, Utsumi F, Nakamura K, *et al*. Possible therapeutic option of aqueous plasma for refractory ovarian cancer. *Clin Plasma Med* 2016; **4**: 14–18.
46 Schilsky RL, Choi KE, Grayhack J, Grimmer D, Guarnieri C, Fullem L. Phase I clinical and pharmacologic study of intraperitoneal cisplatin and fluorouracil in patients with advanced intraabdominal cancer. *J Clin Oncol* 1990; **8**: 2054–2061.
47 McArdle CS, Kerr DJ, O'Gorman P, *et al*. Pharmacokinetic study of 5-fluorouracil in a novel dialysate solution: a long-term intraperitoneal treatment approach for advanced colorectal carcinoma. *Br J Cancer* 1994; **70**: 762–766.
48 Kim JH, Lee JM, Ryu KS, *et al*. Consolidation hyperthermic intraperitoneal chemotherapy using paclitaxel in patients with epithelial ovarian cancer. *J Surg Oncol* 2010; **101**: 149–155.
49 Abu-Elhasan AM, Abdellah MS, Hamed HO. Safety and efficacy of postoperative continuous intra-peritoneal wash with lactated Ringer's for minimizing post-myomectomy pelvic adhesions: a pilot clinical trial. *Eur J Obstet Gynecol Reprod Biol* 2014; **183**: 78–82.